METABOLIC DISEASE

Preclinical efficacy of the GPER-selective agonist G-1 in mouse models of obesity and diabetes

Geetanjali Sharma[1], Chelin Hu[2], Daniela I. Staquicini[3,4], Jonathan L. Brigman[5], Meilian Liu[6,7], Franck Mauvais-Jarvis[8,9], Renata Pasqualini[3,4], Wadih Arap[4,10], Jeffrey B. Arterburn[11], Helen J. Hathaway[2,12], Eric R. Prossnitz[1,7,12]*

Human obesity has become a global health epidemic, with few safe and effective pharmacological therapies currently available. The systemic loss of ovarian estradiol (E2) in women after menopause greatly increases the risk of obesity and metabolic dysfunction, revealing the critical role of E2 in this setting. The salutary effects of E2 are traditionally attributed to the classical estrogen receptors ERα and ERβ, with the contribution of the G protein–coupled estrogen receptor (GPER) still largely unknown. Here, we used ovariectomy- and diet-induced obesity (DIO) mouse models to evaluate the preclinical activity of GPER-selective small-molecule agonist G-1 (also called Tespria) against obesity and metabolic dysfunction. G-1 treatment of ovariectomized female mice (a model of postmenopausal obesity) reduced body weight and improved glucose homeostasis without changes in food intake, fuel source usage, or locomotor activity. G-1–treated female mice also exhibited increased energy expenditure, lower body fat content, and reduced fasting cholesterol, glucose, insulin, and inflammatory markers but did not display feminizing effects on the uterus (imbibition) or beneficial effects on bone health. G-1 treatment of DIO male mice did not elicit weight loss but prevented further weight gain and improved glucose tolerance, indicating that G-1 improved glucose homeostasis independently of its antiobesity effects. However, in ovariectomized DIO female mice, G-1 continued to elicit weight loss, reflecting possible sex differences in the mechanisms of G-1 action. In conclusion, this work demonstrates that GPER-selective agonism is a viable therapeutic approach against obesity, diabetes, and associated metabolic abnormalities in multiple preclinical male and female models.

INTRODUCTION

Diet, lifestyle, and environmental factors have contributed to the global obesity epidemic (*1, 2*). Currently, in the United States, about two-thirds of the population is overweight [body mass index (BMI), >25 kg/m^2], and ~40% are obese (BMI, >30 kg/m^2), proportions that have increased up to threefold in the past ~30 years (*3*). With obesity comes an increased risk of metabolic syndrome (namely, diabetes, arterial hypertension, and cardiovascular disease), stroke, and cancer. To date, few treatments have been successful in counteracting or reversing obesity, with most acting through the central nervous system to regulate satiety or satiation through appetite suppression (*1*). Of the U.S. Food and Drug Administration–approved weight loss drugs, several have been withdrawn because of unexpected tox-icity (for example, fenfluramine and sibutramine) or have undesirable side effects such as steatorrhea in the case of lipase inhibitors (for example, orlistat) (*4*). Approaches using vascular targeting of adipose tissue such as adipotide have shown promise (*5, 6*) but remain investigational. Glucagon-like peptide-1 (GLP-1) receptor agonists (for example, liraglutide and semaglutide), originally designed to treat diabetes (*7*), have recently shown efficacy in obesity, although not without side effects (*8*). Unfortunately, "effective" marketed drugs only result in sustained weight loss of typically ~5%, even with patients adhering to strict diets, due in part to adaptive thermogenesis or metabolic adaptation (*9*). Thus, it is imperative to identify targets, pathways, and drug classes to treat obesity and its associated complications (*10*).

The main female estrogen 17β-estradiol (E2) exerts sexually dimorphic protective effects on metabolism and cardiovascular physiology through diverse molecular and cellular pathways (*11*), preventing visceral obesity, hyperlipidemia, insulin resistance, inflammation, and hypertension in premenopausal women compared to age-matched men (*12–14*). Thus, postmenopausal women exhibit an increased susceptibility to weight gain and associated metabolic dysfunction due to the loss of estrogenic protection, which can be ameliorated by E2 supplementation (*14*). The metabolic effects of E2 have been largely attributed to the nuclear estrogen receptors α and β (ERα and ERβ) that conventionally function as ligand-activated transcription factors (*15*), although rapid signaling in response to E2 has become recognized as critical to overall estrogenic activities (*16–18*). On the basis of both genetic and pharmacological approaches, an accumulating body of evidence reveals that the G protein–coupled estrogen receptor (GPER; previously known as GPR30) plays an important role in the actions of E2 and, specifically, the regulation of metabolism, as well as cardiovascular function and cancer (*19–24*).

[1]Division of Molecular Medicine, Department of Internal Medicine, University of New Mexico Health Science Center, Albuquerque, NM 87131, USA. [2]Department of Cell Biology and Physiology, University of New Mexico Health Science Center, Albuquerque, NM 87131, USA. [3]Division of Cancer Biology, Department of Radiation Oncology, Rutgers New Jersey Medical School, Newark, NJ 07103, USA. [4]Rutgers Cancer Institute of New Jersey, Newark, NJ 07103, USA. [5]Department of Neurosciences, University of New Mexico Health Science Center, Albuquerque, NM 87131, USA. [6]Department of Biochemistry and Molecular Biology, University of New Mexico Health Science Center, Albuquerque, NM 87131, USA. [7]Center of Biomedical Research Excellence in Autophagy, Inflammation and Metabolism, University of New Mexico Health Science Center, Albuquerque, NM 87131, USA. [8]Diabetes Discovery and Sex-Based Medicine Laboratory, Section of Endocrinology and Metabolism, Department of Medicine, Tulane University Health Sciences Center, School of Medicine, New Orleans, LA 70112, USA. [9]Section of Endocrinology, Southeast Louisiana Veterans Administration Health Care System, New Orleans, LA 70112, USA. [10]Division of Hematology/Oncology, Department of Medicine, Rutgers New Jersey Medical School, Newark, NJ 07103, USA. [11]Department of Chemistry and Biochemistry, New Mexico State University, Las Cruces, NM, 88003, USA. [12]University of New Mexico Comprehensive Cancer Center, University of New Mexico Health Science Center, Albuquerque, NM 87131, USA.
*Corresponding author. Email: eprossnitz@salud.unm.edu

Our previous studies have shown that male GPER knockout (KO) mice recapitulate many aspects of metabolic syndrome, including obesity, increased gonadal fat pad mass, dyslipidemia, insulin resistance, glucose intolerance, and inflammation (25). GPER KO mice exhibit a sexual temporal dimorphism, in which male GPER KO mice gain weight earlier than female GPER KO mice, although both male and female GPER KO mice show marked reductions in energy expenditure and expression of thermogenic genes in brown fat (26). Furthermore, female (but not male) GPER KO mice were less sensitive to the anorectic effects of leptin and cholecystokinin compared to isogenic wild-type (WT) mice, and E2 supplementation of ovariectomized (OVX) GPER KO mice did not reduce body weight (26). Together, these findings provide strong evidence that E2 may regulate body weight and metabolism, at least in part, via known and perhaps as yet unknown GPER-mediated mechanisms.

In this study, we report the metabolic effects and therapeutic benefits of selective GPER activation in vivo. We used both OVX female mice, as a model of postmenopausal E2 loss, and diet-induced obesity (DIO) in male and OVX female mice, all of which exhibit weight gain and metabolic dysfunction. Because E2 binds nonselectively to all three receptors (ERα, ERβ, and GPER), we selectively activated GPER using its only known highly selective small-molecule (molecular mass, 412.3 Da) agonist, G-1 (27–32). Our results demonstrate that GPER activation by G-1 may represent a translational approach by a lead prototype agent in the treatment of human obesity and aspects of metabolic syndrome, particularly diabetes, in postmenopausal women and in men.

RESULTS

GPER activation reduces obesity resulting from estrogen deficiency

Previous studies from our group (25, 33, 34) and other investigators (35) have shown that GPER deficiency in mice results in obesity with concomitant disturbances in glucose and lipid homeostasis, although one report has found the opposite (36). Thus, we sought to determine whether activation of GPER in E2-deficient mice can alleviate obesity and symptoms of metabolic dysfunction in this setting. To address this possibility, we used an OVX mouse model in which bilateral surgical removal of the ovaries, resulting in the marked loss of endogenous E2, leads to multiple aspects of metabolic dysfunction, similar to that in either surgically or naturally (age-related) postmenopausal women. In our study, female mice were OVX at 10 weeks of age (mean body weight, 22.5 ± 1.6 g) and allowed feeding ad libitum on normal chow (NC) for an additional 12 weeks. At this point, the difference between the mean body weights of ovary-intact and OVX cohorts of mice was 5.3 g (29.2 ± 0.8 g versus 34.5 ± 2.8 g, respectively; $P < 0.01$), an increase of about 18% body weight in the OVX cohort (Fig. 1A). Furthermore, the OVX mice also displayed impaired glucose homeostasis as revealed by elevated baseline blood glucose and impaired glucose and insulin tolerance (fig. S1). Subsequently, OVX mice were randomized into two cohorts treated with either the GPER-selective agonist G-1 or vehicle for an additional 6 weeks and compared to an age-matched cohort of ovary-intact mice.

During the 6-week G-1 treatment period, body weights were measured weekly. Whereas ovary-intact mice demonstrated a slight
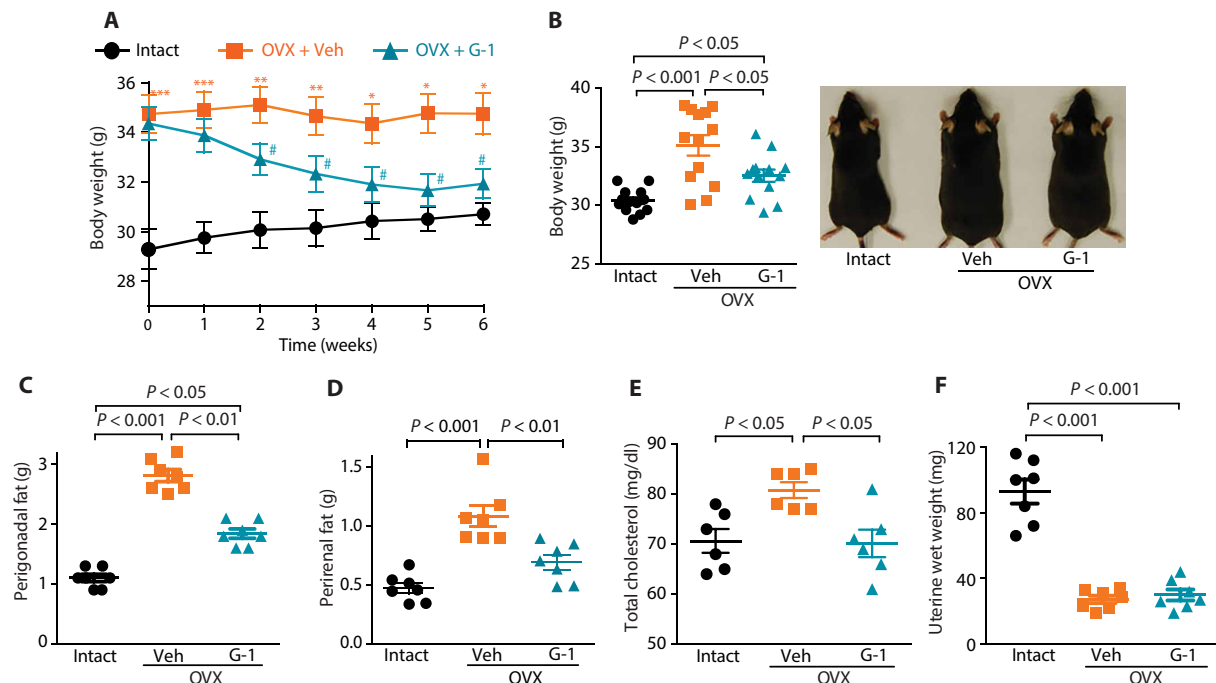

Fig. 1. Selective activation of GPER in OVX mice attenuates obesity. Body weight in OVX mice after treatment with GPER agonist G-1 compared to vehicle (Veh) controls and ovary-intact mice (**A**) over time and (**B**) at termination of the study. Images of representative mice are shown in (B). The weight of the perigonadal (**C**) and perirenal (**D**) fat pads, circulating cholesterol (**E**), and uterine wet weight (**F**) were determined at termination of the study. (A) $n = 5$ (intact) to 14 (OVX + Veh and OVX + G-1), (B) $n = 13$, (C, D, and F) $n = 7$, and (E) $n = 6$. (A) Two-way ANOVA; *$P < 0.05$, **$P < 0.01$, and ***$P < 0.001$ for vehicle treatment versus ovary intact controls, respectively; #$P < 0.05$ for G-1 treatment versus vehicle treatment. (B to F) One-way ANOVA with Bonferroni post hoc test.

increase in weight from 29.2 ± 0.8 g to 30.7 ± 0.4 g (*P* = not significant), vehicle-treated OVX mice did not exhibit any detectable changes in weight (Fig. 1A). In contrast, G-1 treatment of OVX mice led to a progressive loss of body weight, first detectable at 2 weeks of treatment (vehicle, 35.1 ± 0.7 g, versus G-1, 32.9 ± 0.6 g; *P* < 0.05). From that point forward, G-1–treated mice continued to lose weight, such that by 4 weeks of treatment, their weights were similar to those of ovary-intact animals (intact, 30.4 ± 0.7 g, versus G-1 treatment, 31.8 ± 0.7 g; *P* = 0.25), similar to that observed at termination of the experiment when mice were euthanized (Fig. 1B).

At the end of the treatment period, dissection of perigonadal (Fig. 1C) and perirenal (Fig. 1D) fat pads revealed that G-1 reduced the wet weights of both fat pads in OVX mice. Because obesity results in dyslipidemia, we also analyzed fasting circulating plasma lipids, which revealed that ovariectomy increased total cholesterol in mice and that G-1 treatment markedly reduced cholesterol in OVX mice to concentrations of ovary-intact control mice (Fig. 1E). Triglycerides, however, were not statistically different between any treatment cohorts (ovary intact, 63.1 ± 3.8 mg/dl; OVX + vehicle, 62.8 ± 4.4 mg/dl; OVX + G-1, 60.8 ± 5.6 mg/dl). Because E2 treatment is known to promote uterotrophic actions such as imbibition (an increase in wet weight) in OVX mice, uterine wet weights were

also determined. As expected, ovariectomy resulted in a substantial decrease in uterine wet weight; however, G-1 treatment had no effect on uterine wet weight when compared to vehicle-treated OVX mice (Fig. 1F), extending our previous observations that acute G-1 treatment does not promote the classical feminizing reproductive effects resulting from E2 treatment (*28*).

Analysis of body composition as determined by dual-energy x-ray absorptiometry (DEXA) and magnetic resonance imaging (MRI) confirmed a marked increase in body fat upon ovariectomy, with G-1 treatment substantially reducing overall fat in OVX mice (Fig. 2). DEXA scans revealed lower body fat content (Fig. 2, A and B) and body fat percentage (Fig. 2C) in G-1–treated OVX mice without any changes in lean mass (Fig. 2D), bone mineral density (Fig. 2E), or bone mineral content (Fig. 2F) in comparison to vehicle-treated OVX mice. However, ovary-intact mice had higher bone mineral density and bone mineral content as compared to either vehicle- or G-1–treated OVX cohorts, indicating that G-1 is not effective, thereby differing from E2 (*37*), in preventing bone loss (Fig. 2, E and F). Furthermore, quantitation of fat-water MRI images revealed that whereas OVX increases overall abdominal (Fig. 2, G and H) and subcutaneous fat (Fig. 2, I and J), G-1 treatment led to a loss of fat in both fat depots to amounts near to those of ovary-intact mice.
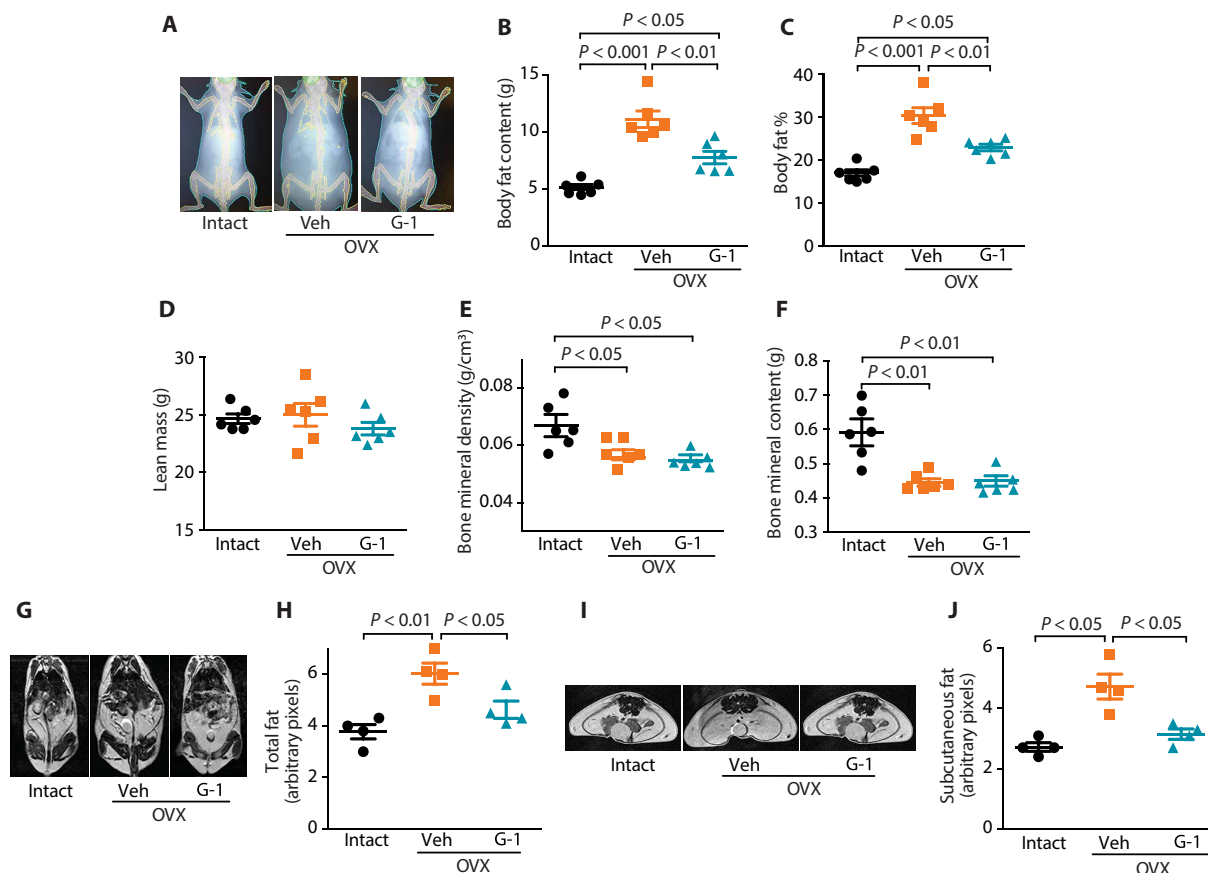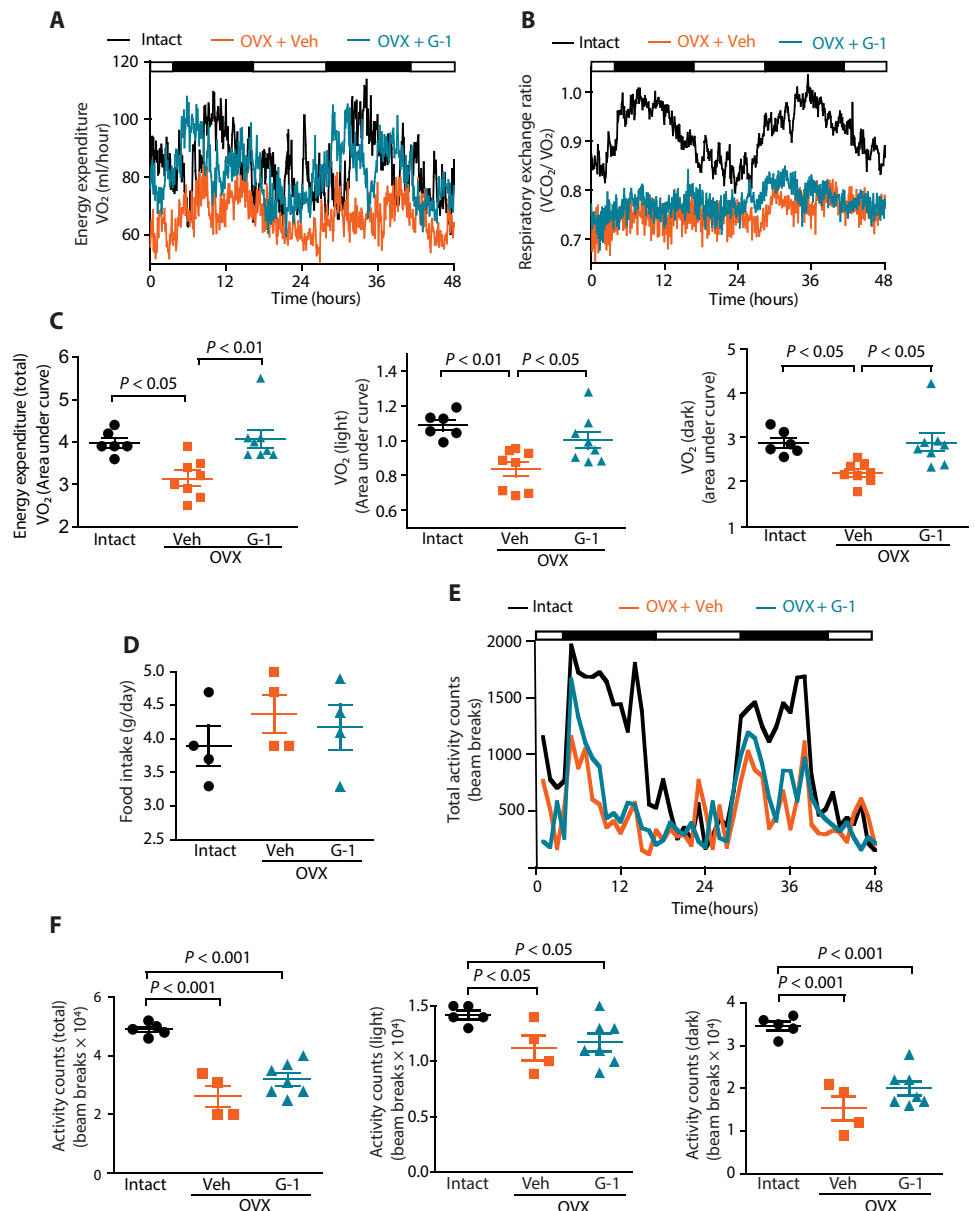
Fig. 2. Treatment with GPER-selective agonist G-1 reduces fat content in OVX mice. (**A**) Representative DEXA scans, (**B**) overall body fat content, (**C**) body fat percentage, (**D**) lean mass, (**E**) bone mineral density, and (**F**) bone mineral content in vehicle- and G-1–treated OVX mice compared to ovary-intact animals. Representative anatomical MRI images of the (**G**) coronal and (**I**) axial view in different mouse cohorts with quantification of (**H**) total (from coronal view) and (**J**) subcutaneous (from axial view) fat content. (B to F) *n* = 6 and (H and J) *n* = 4. All tests are one-way ANOVA with Bonferroni post hoc test.

OVX mice exhibit increased energy expenditure after G-1 treatment

Lower body weight and decreased fat accumulation as observed with G-1 treatment could have resulted from either reduced caloric intake or increased energy expenditure, which itself may be the result of either enhanced basal metabolic rate or locomotion. To differentiate between these possibilities, we placed mice in metabolic cages to measure food intake, energy expenditure (measured as VO_2), and respiratory exchange ratio [RER; the ratio of carbon dioxide production (VCO_2) divided by oxygen consumption (VO_2)]. RER provides an estimate of the fuel source used for energy production based on the difference in the amount of oxygen required for glucose versus fatty acid oxidation. An RER value of ~0.7 indicates that fat is the predominant fuel source, with a value of ~0.85 suggesting a mix of fat and carbohydrates, and an RER value of ~1 or above indicating carbohydrate as the predominant fuel source (38). Compared to ovary-intact mice, vehicle-treated OVX mice showed a marked reduction in energy expenditure, RER, and locomotor activity during both the light and dark cycles, with no detectable effects on food intake (Fig. 3, A to F). However, G-1–treated OVX mice displayed increased energy expenditure in both light and dark cycles compared to vehicle-treated mice (Fig. 3, A and C), but the RER did not change (ranging between 0.7 and 0.85), suggesting a mix of carbohydrates and fat as the energy source. In contrast, the RER for ovary-intact mice during dark cycle was close to 1, indicating carbohydrate as the primary energy source (Fig. 3B). Furthermore, G-1 had no effect on food intake (Fig. 3D) or locomotor activity (Fig. 3, E and F) in OVX mice compared to vehicle controls. Together, these results demonstrate that G-1 treatment increases energy expenditure using fat as one of the main energy sources in the absence of effects on food intake or locomotor activity.

Fig. 3. GPER activation in OVX mice increases energy expenditure. (**A**) Energy expenditure over time (VO_2; milliliter/hour), (**B**) RER over time (VCO_2/VO_2), (**C**) oxygen consumption (VO_2; total, light and dark phases), (**D**) food intake, and (**E**) locomotor activity over time and (**F**) total, light and dark phases, in vehicle- and G-1–treated OVX mice compared to the ovary-intact control animals. (A to C) $n = 6$ (intact) to 8 (OVX + Veh and OVX + G-1) and (D to F) $n = 4$ to 7. All tests are one-way ANOVA with Bonferroni post hoc test.

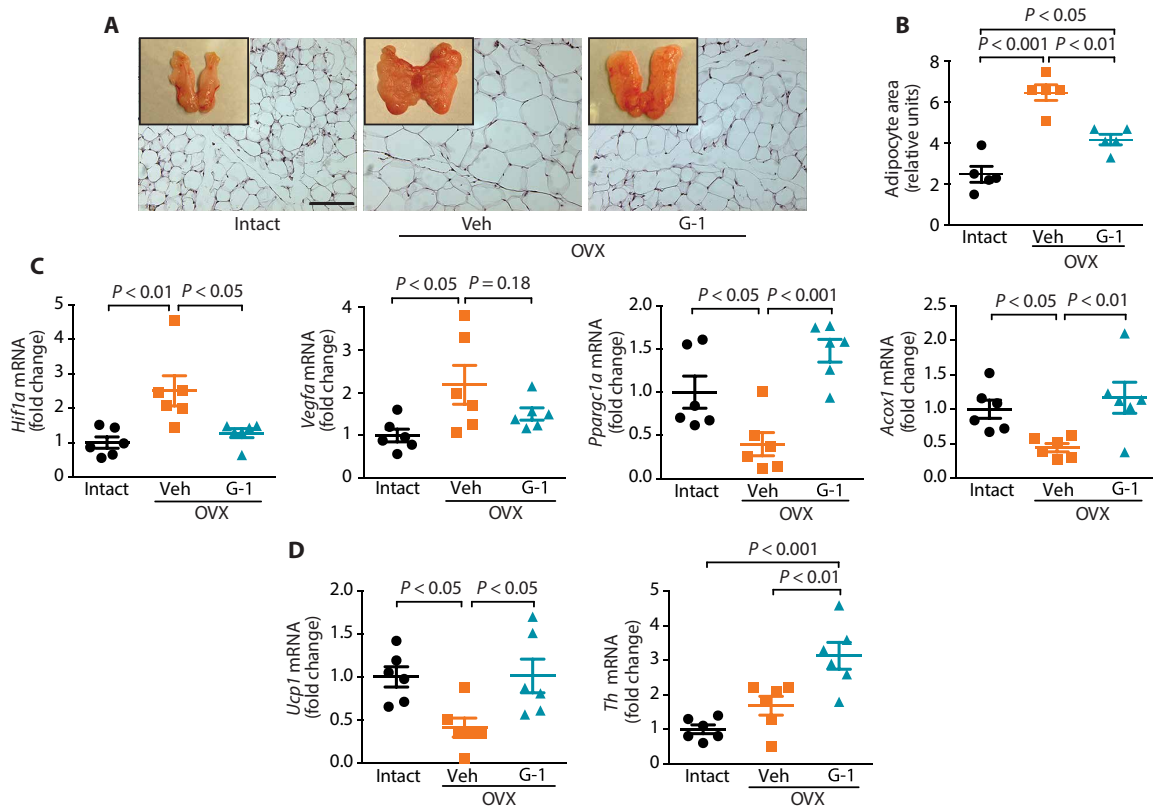## Adipose tissue remodeling in OVX mice after G-1 treatment

The attenuation of obesity and enhanced energy expenditure (Fig. 3) after G-1 treatment in OVX mice suggests that the GPER agonist exerts these beneficial effects in part through modulation of adipose tissue. Adipose tissue undergoes marked metabolic and functional changes during obesity, including an increase in the size of adipocytes, hypoxia, inflammation, and changes in glucose and lipid metabolism (39, 40). OVX mice treated with vehicle alone exhibited an increase in the size of both the overall fat pad and individual adipocytes (Figs. 1C and 4, A and B). In addition to reducing the overall weight and size of the perigonadal fat pad, G-1 treatment also reduced the size of individual adipocytes relative to vehicle-treated OVX mice (Fig. 4, A and B), indicating enhanced metabolism in adipose tissue.

Obesity leads to adipose tissue expansion by modulating the expression of key genes involved in hypoxia and angiogenesis (39, 41). We therefore investigated whether G-1 treatment modulates the expression of genes involved in multiple aspects of adipose function. Gene expression of peroxisome proliferator–activated receptor

Fig. 4. Adipose tissue remodeling in OVX mice treated with GPER-selective agonist G-1. (**A**) Perigonadal fat pads (whole mount and H&E-stained sections; scale bar, 100 μm) and (**B**) mean adipocyte area as quantified after H&E staining in (A) ($n = 5$). (**C**) Gene expression analyses in perigonadal WAT for genes involved in angiogenesis (*Hif1a* and *Vegfa*) and mitochondrial biogenesis (*Ppargc1a*) and fatty acid oxidation (*Acox1*) ($n = 6$). (**D**) Gene expression analyses in BAT for genes involved in thermogenesis (*Ucp1*) and sympathetic innervation (*Th*) ($n = 6$). Statistical significance was determined by one-way ANOVA with Bonferroni post hoc test.

γ coactivator 1α (PGCα) (*Ppargc1a*; a regulator of cellular energy metabolism), peroxisomal acyl–coenzyme A (co-A) oxidase (*Acox1*; which catalyzes fatty acid β-oxidation), hypoxia-inducible factor 1α (*Hif1a*), and vascular endothelial growth factor A (*Vegfa*), the latter two being important mediators of angiogenesis and tissue expansion, was analyzed by reverse transcription quantitative polymerase chain reaction (RT-qPCR) (*39*, *41*). OVX increased the expression of angiogenic genes (*Hif1a* and *Vegfa*) with a concomitant decrease in the expression of genes involved in oxidative metabolism (*Ppargc1a* and *Acox1*) in the perigonadal fat pad, whereas G-1 generally normalized these altered gene expression patterns (Fig. 4C). We also analyzed the brown adipose tissue (BAT) gene expression of uncoupling protein1 (*Ucp1*), which is implicated in conferring the thermogenic ability of BAT (*42*). OVX substantially reduced *Ucp1* expression, with G-1 treatment restoring its expression (Fig. 4D). BAT thermogenesis is also regulated by the central nervous system through innervation of BAT. To test whether G-1 might be acting on BAT through indirect mechanisms, we quantified the gene expression of tyrosine hydroxylase (*Th*), the rate-limiting enzyme in norepinephrine synthesis and thus a marker for sympathetic innervation. *Th* expression was higher in the BAT from OVX mice treated with G-1 compared to either ovary-intact mice or vehicle-treated OVX mice (Fig. 4D). Together, these results suggest that activation of GPER to increase thermogenesis in BAT, which increases energy expenditure and ultimately enhances white adipose tissue (WAT) catabolism, decreasing body weight, is a central mechanism to our observations.

Up-regulation of mitochondrial gene expression and increased cellular respiration with G-1 treatment

Because we observed an increase in whole-body energy expenditure in mice after G-1 treatment, we examined mitochondrial gene expression in metabolically important tissues that use or dissipate energy, such as BAT and skeletal muscle. Our results demonstrate an increase in the expression of mitochondrial genes including *Ppargc1a* and its downstream targets acetyl co-A carboxylase α (*Acaca*), nuclear respiratory factor 1 (*Nrf1*), and transcriptional factor A mitochondrial (*Tfam*) in BAT upon G-1 treatment of OVX mice (Fig. 5A). These mitochondrial genes regulate oxidative metabolism and maintain glucose and lipid homeostasis and energy balance. Similarly, gene expression of *Acaca*, *Nrf1*, *Tfam*, and *Acox1* was also up-regulated in the skeletal muscle of G-1–treated mice (Fig. 5B). Up-regulation of these mitochondrial genes in BAT and skeletal muscle suggests increased fuel utilization, in particular, through β-oxidation.

To test further whether G-1 leads to increased cellular metabolism, we quantified respiration in brown preadipocytes in vitro. Stimulation of GPER with G-1 for 24 hours resulted in a higher basal oxygen consumption rate (OCR) and increased maximal cellular respiration in response to the mitochondrial uncoupling agent carbonyl cyanide-4-trifluoromethoxyphenylhydrazone (FCCP) (Fig. 5C). Oxygen consumption in response to oligomycin, which inhibits adenosine 5′-triphosphate (ATP) synthesis, and rotenone/antimycin A, which block all electron transport, was similar in both groups. On the basis of these results, basal and maximal respiration, spare respiratory

Sharma *et al.*, *Sci. Transl. Med.* **12**, eaau5956 (2020)   29 January 2020

5 of 14
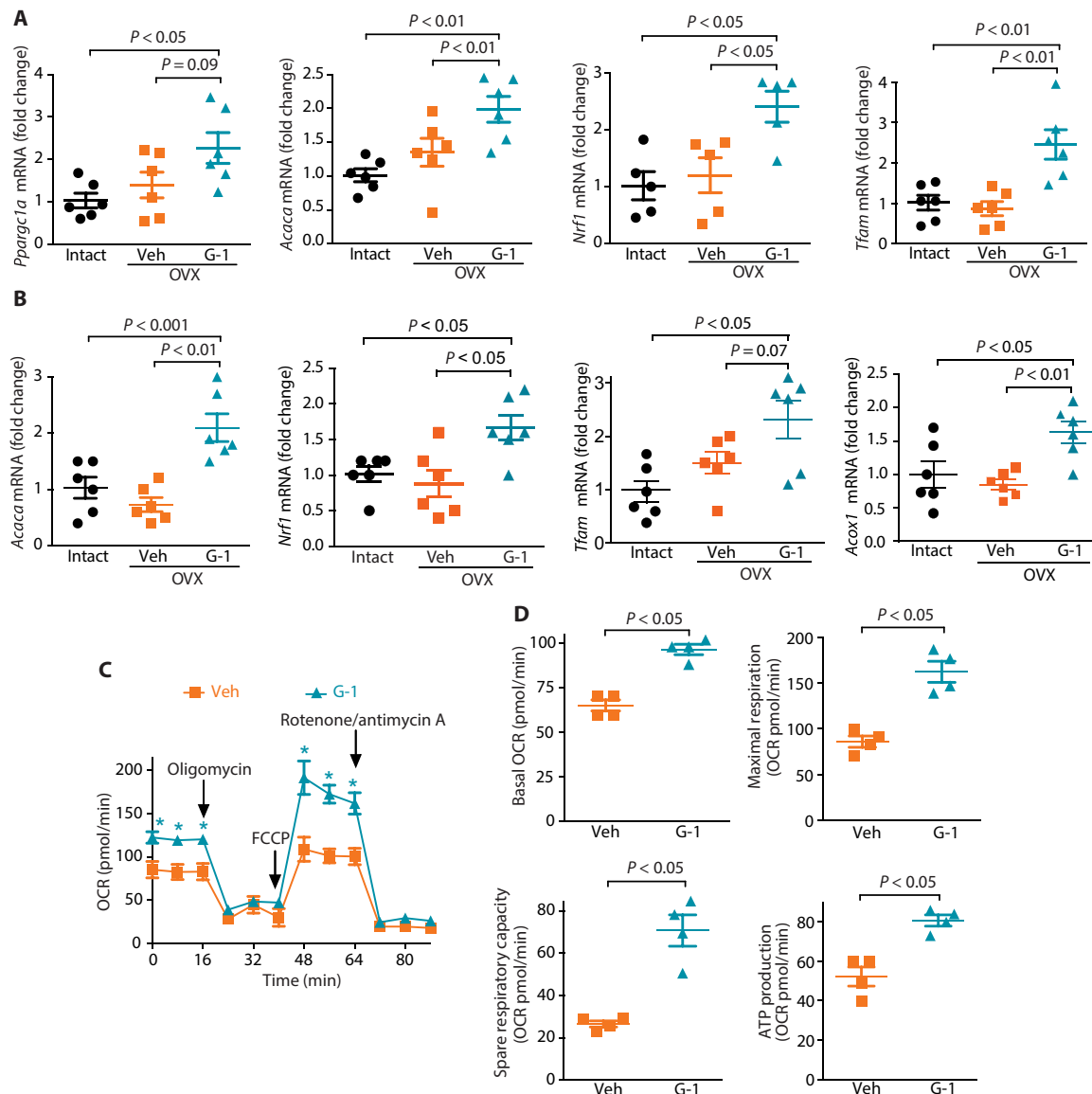
Fig. 5. G-1 treatment increases mitochondrial gene expression and cellular respiration. Expression of the mitochondrial genes *Ppargc1a*, *Acaca*, Nrf1, *Tfam*, and *Acox1* in (**A**) BAT and (**B**) skeletal muscle after vehicle or G-1 treatment of OVX mice (*n* = 5 to 6). (**C**) Oxygen consumption rate (OCR) of brown preadipocytes under basal conditions (0 to 16 min) after GPER stimulation for 24 hours with 100 nM G-1.*P < 0.001 for G-1–treated cells versus vehicle control. (**D**) Basal OCR, maximal OCR, spare respiratory capacity, and OCR for ATP production in G-1–treated cells versus control cells. The results shown in (C) and (D) are representative of three independent experiments with four replicates for each condition per experiment as indicated. Statistical significance was determined by (A and B) one-way ANOVA with Bonferroni post hoc test, (C) two-way ANOVA, and (D) Mann-Whitney *U* test.

capacity, and respiration toward ATP production were all increased with G-1 treatment (Fig. 5D), revealing that GPER stimulation enhanced mitochondrial function in brown preadipocytes in vitro, consistent with the observed increases in BAT gene expression and increased energy expenditure observed in vivo. Together, these results suggest that activation of GPER enhances adipose tissue metabolism and energy expenditure, which, together, lead to weight loss.

GPER agonism alleviates inflammation in OVX mice
Increased body weight and dyslipidemia lead to systemic inflammation and dysregulation of metabolic homeostasis. Because OVX mice exhibited increased obesity and higher circulating lipids, we next assessed the systemic concentrations of inflammatory cytokines [tumor

necrosis factor–α (TNFα), monocyte chemotactic protein 1 (MCP1), and interleukin-6 (IL6)] in plasma and gene expression of multiple markers of inflammation (*Tnf*, TNFα; *Ccl2*, MCP1; and *Adgre1*, F4/80) in the perigonadal adipose tissue, liver, and skeletal muscle. Our results revealed that OVX led to increased circulating TNFα, MCP1, and IL6, which were reduced upon G-1 treatment (Fig. 6A). Furthermore, the OVX-induced increase in mRNA expression of inflammatory markers was diminished by G-1 to varying extents in the perigonadal adipose tissue (Fig. 6B), liver (Fig. 6C), and skeletal muscle (Fig. 6D). These results reveal that G-1 reverses the inflammatory pathophysiological phenotype in OVX mice, likely contributing to the normalization of metabolic dysfunction in multiple tissues.
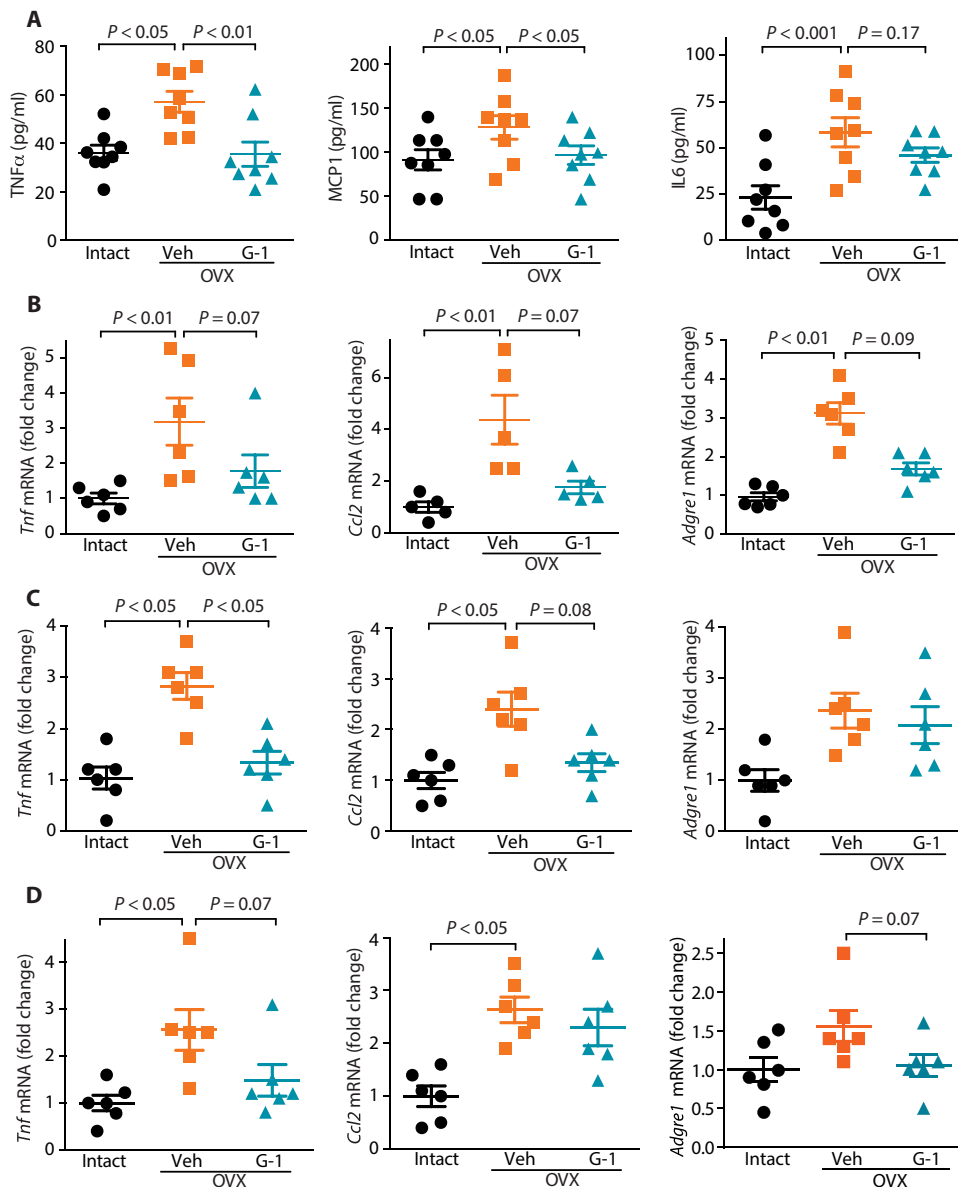
Fig. 6. GPER agonism attenuates inflammation resulting from OVX. (**A**) Systemic concentrations of inflammatory cytokines ($n = 8$). Gene expression of inflammatory markers in (**B**) perigonadal WAT, (**C**) liver, and (**D**) skeletal muscle ($n = 5$ to 6). Statistical significance was determined by one-way ANOVA with Bonferroni post hoc test.

clearance (Fig. 7, A and B). In addition, whereas OVX also increased fasting blood glucose and insulin concentrations, resulting in an elevated homeostatic model assessment of insulin resistance (HOMA-IR) index, G-1 treatment led to a decrease in fasting glucose and insulin concentrations (Fig. 7, C to D) with a concomitant decrease in the HOMA-IR index (Fig. 7E).

Body weight and metabolic regulation are driven by a complex interplay between multiple hormones that participate in key metabolic functions, including satiety and satiation, insulin sensitivity, and glucose and lipid homeostasis (*43*, *44*). OVX led to increased plasma resistin, leptin, insulin, pancreatic polypeptide (PP), C-peptide 2, and glucagon as hallmarks of obesity and metabolic dysfunction, with G-1 treatment decreasing all except glucagon (Fig. 7F). Neither OVX nor G-1 had effects on ghrelin, peptide YY (PYY), gastric inhibitory polypeptide (GIP), amylin, or GLP-1 (fig. S2). These results demonstrate that G-1 has the capacity to regulate multiple aspects of metabolism by modulating glucose homeostasis and several metabolic hormones.

G-1 reduces weight gain and improves glucose homeostasis in DIO mice

To determine whether G-1 might also be effective in DIO models, we first fed male mice a high-fat diet (HFD) for 12 weeks to induce obesity (Fig. 8A), glucose intolerance, and insulin resistance (fig. S3) and subsequently treated mice for 8 weeks with G-1. Compared to G-1–treated OVX female mice that lost weight over time (Fig. 1A), G-1 treatment in male mice prevented further weight gain, with con-

GPER activation in OVX mice improves glucose homeostasis and metabolic hormone profiles

Increased obesity resulting from OVX leads to metabolic dysfunction due to multiple factors including ectopic lipid accumulation and inflammation, which, in turn, lead to insulin resistance and reduced glucose tolerance. Because treatment of OVX mice with G-1 reduced obesity, we sought to determine whether G-1 treatment also improves glucose homeostasis. To this end, we performed glucose tolerance tests (GTTs) to assess glucose clearance from blood and quantified fasting glucose and insulin as measures of glucose homeostasis in vivo. Compared to ovary-intact control mice, OVX led to delayed glucose clearance in the vehicle-treated mice (Fig. 7, A and B), similar to the baseline values before treatment (fig. S1). With G-1 treatment, OVX mice exhibited a marked improvement in glucose

trol (vehicle-treated) male mice continuing to gain weight over the course of treatment (Fig. 8A). At the end of the 8-week treatment period, compared to vehicle-treated mice, G-1–treated male mice exhibited reduced plasma cholesterol (Fig. 8B) and increased energy expenditure (Fig. 8C) to levels similar to those observed in male mice fed NC. Unexpectedly, although G-1–treated male mice did not exhibit any overall weight loss over the 8-week treatment period, fasting glucose (Fig. 8D) and insulin (Fig. 8E), HOMA-IR (Fig. 8F), and glucose tolerance (Fig. 8, G and H) were all markedly improved. Thus, whereas improved glucose homeostasis in G-1–treated OVX female mice correlated with weight loss, in obese male mice, the improved glucose homeostasis occurred in the absence of overall weight loss. Because diet often contributes to obesity and diabetes in postmenopausal women, we further extended
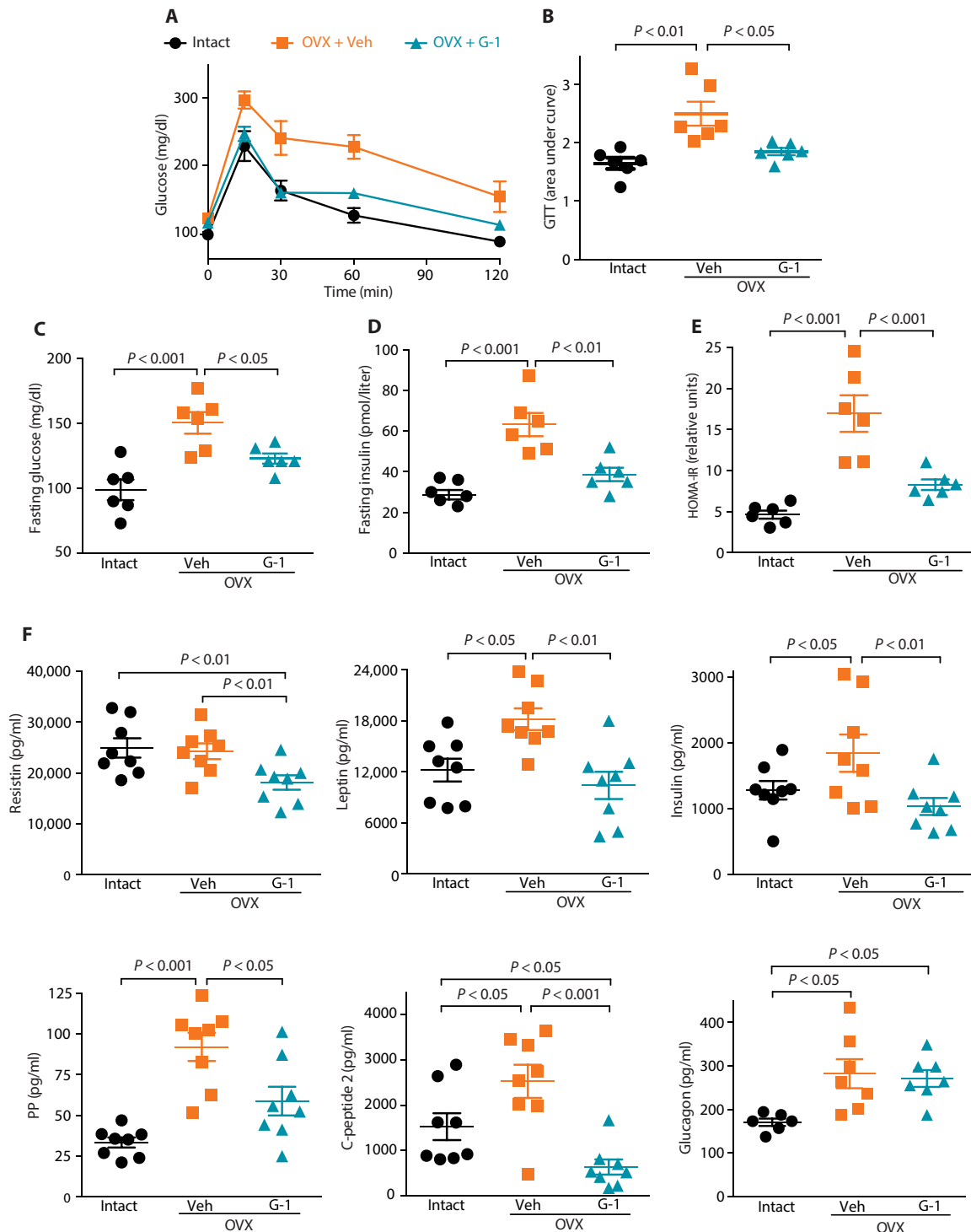
Fig. 7. GPER-selective agonist G-1 improves glucose homeostasis in OVX mice and modulates systemic concentrations of metabolic hormones. (**A** and **B**) Tolerance to glucose (glucose tolerance test, GTT); fasting plasma (**C**), glucose, and (**D**) insulin; and (**E**) HOMA-IR in vehicle- and G-1–treated OVX mice compared to ovary-intact mice. For GTT, area under the curve for each individual mouse in (A) was plotted in (B). (**F**) Concentrations of plasma leptin, insulin, pancreatic polypeptide (PP), C-peptide 2, and glucagon in the fed state. (A to E) $n = 6$ and (F) $n = 6$ to 8. Statistical significance was determined by one-way ANOVA with Bonferroni post hoc test.

our observations with OVX female mice by adding an HFD to determine whether G-1 could alleviate the combined deleterious effects of estrogen deprivation and HFD. Under these conditions, G-1 treatment significantly decreased body weight and improved

glucose homeostasis in OVX/HFD mice (fig. S4). Thus, our studies provide strong evidence that G-1 exerts antiobesity and antidiabetic effects across multiple preclinical models of obesity and diabetes in both males and females.
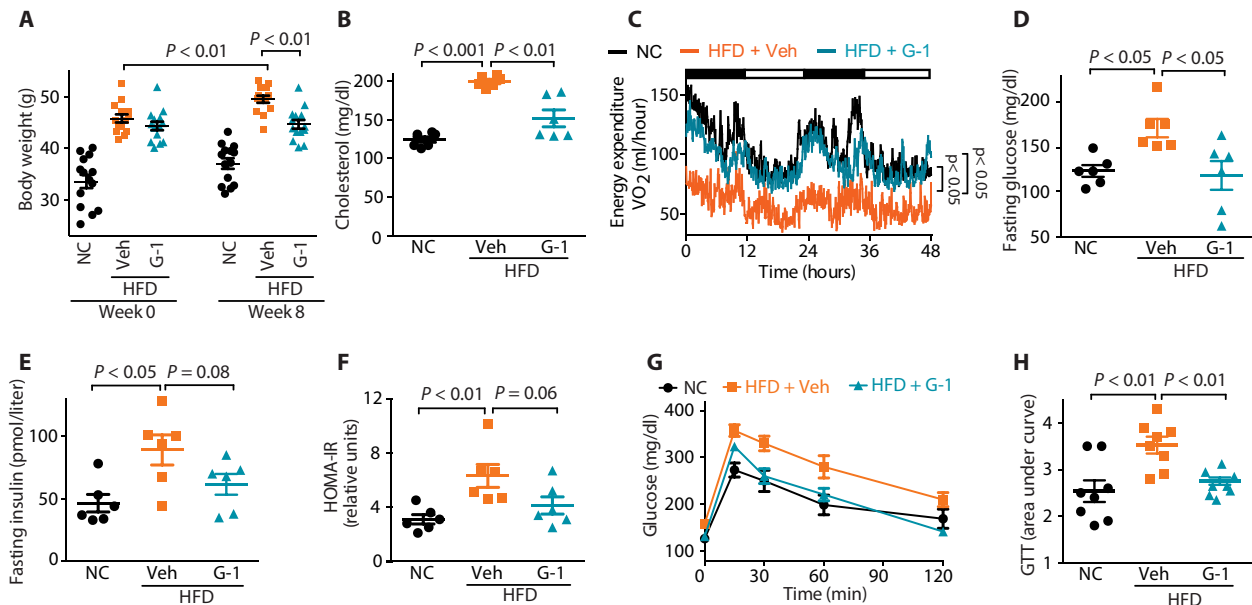
Fig. 8. Activation of GPER by G-1 exerts antiobesity and antidiabetic effects in male DIO mice. (**A**) Body weights ($n = 14$), (**B**) plasma cholesterol concentrations ($n = 6$), (**C**) energy expenditure ($n = 4$), fasting (**D**) glucose ($n = 6$) and (**E**) insulin ($n = 6$) concentrations, (**F**) HOMA-IR ($n = 6$), and (**G** and **H**) glucose tolerance ($n = 8$) in DIO male mice treated with vehicle or G-1 compared in male mice fed normal chow (NC). For (D) and (H), area under the curve was determined for each individual mouse in (C) and (G), respectively. Statistical significance was determined by one-way ANOVA with Bonferroni post hoc test.

DISCUSSION

In the present study, we used various models of obesity and diabetes to determine the impact of selective GPER agonism on multiple aspects of metabolism, including body weight regulation and obesity, bone health, glucose and lipid homeostasis, and hormone/cytokine regulation. We and others have shown that GPER deficiency results in phenotypic abnormalities similar to those observed in mice lacking ERα with regard to metabolism, including obesity, dyslipidemia, insulin resistance, glucose intolerance, and inflammation (*19, 25, 26, 35, 45–47*). These observations suggest a potential overlap or synergy in the metabolic functions carried out by both receptors. Our central objective was to determine whether selective GPER activation would effectively treat obesity and its associated pathologies in E2-deficient female mice as well as in DIO in male and E2-deficient female mice. Our results establish an unrecognized role for the GPER agonist G-1 (a first-in-class prototype drug candidate) in counteracting obesity and metabolic dysfunction resulting from E2 deficiency and DIO, both alone and in combination.

Under our experimental conditions, G-1 reduced body weight in OVX mice due to fat loss as opposed to changes in lean mass. Consistent with a critical role of E2 acting on GPER in the regulation of body weight and obesity, OVX GPER KO mice, unlike their OVX WT counterparts, showed no reductions in body weight upon E2 treatment (*26*). However, the male mice in our DIO experimental paradigm differed from E2-deficient female mice in their response to G-1, lacking further weight gain (which continued in the control male cohort), but with no weight loss as observed in our OVX NC female model. These findings are similar to and consistent with a report in which male mice fed an HFD and treated with E2 ceased gaining weight over time relative to the control diet, whereas the control DIO mice continued to gain weight (*48*).

GPER deficiency leads to increased circulating lipids (*25*), consistent with our current findings that G-1–mediated activation of

GPER lowers total plasma cholesterol. Similar to GPER deficiency in mice, individuals in a cohort of Northern European descent carrying a hypofunctional P16L genetic variant of GPER display increased plasma low-density lipoprotein (LDL) cholesterol (*49*), suggesting potential translational relevance for patients. Our observations that selective GPER agonism not only reverses obesity but also improves plasma lipid profiles demonstrate a potentially important additional therapeutic benefit of G-1 administration.

Maintenance of stable body weight depends on the balance between energy intake and expenditure. Possible mechanisms promoting energy expenditure include a higher metabolic rate and increased respiratory uncoupling (*50*). In this study, GPER activation by G-1 specifically reversed the decrease in energy expenditure due to either OVX or HFD. This result is consistent with findings where GPER deficiency resulted in reduced energy expenditure in both male and female mice (*26*). Our investigation of a molecular basis of the increased energy expenditure in an OVX mouse model revealed that expression of *Ucp1*, and to a lesser extent *Ppargc1a* (which upregulates *Ucp1* expression), was increased in BAT from G-1–treated female mice. Furthermore, our observation of increased *Th* expression with G-1 treatment suggests that G-1 may also exert centrally mediated thermogenic effects in BAT via activation of the sympathetic nervous system (*51*). Consistent with our observations, BAT from GPER-deficient mice exhibited decreased expression of two thermogenic genes, *Ucp1* and *Adrb3* (β₃-adrenergic receptor) (*26*). These collective observations reveal that GPER is a relevant mediator of energy balance in vivo.

Adipose tissue is a central regulator of energy balance and metabolic homeostasis, with the loss of E2 leading to visceral adipose tissue accumulation and dysregulation (*52, 53*). Our results show that G-1 reduced the size of individual adipocytes from WAT, which is known to correlate with increased insulin sensitivity (*54*). Increased adipocyte size can lead to a hypoxic environment, inflammation,

and mitochondrial dysfunction (*39*). Thus, reduced adipocyte size may diminish hypoxia and inflammation. Our results support this hypothesis, as G-1 reduced WAT expression of hypoxia-responsive genes, suggesting that GPER stimulation mitigates hypoxia in WAT. Hypoxia is strongly correlated with increases in circulating leptin and resistin concentrations, along with reduced expression of PGC1α (*41*). Our results establish that G-1 exerts effects similar to those of E2, up-regulating genes involved in mitochondrial biogenesis to promote fat oxidation in WAT and counteract obesity (*55*). We also observed a reduction in circulating concentrations of leptin and resistin upon G-1 treatment, which may contribute to the overall increase in energy expenditure (*56, 57*) and improved glucose homeostasis (*58*). These data are in agreement with reports in which postmenopausal women treated with E2 had lower serum leptin (*59*). Adipose tissue in postmenopausal women exhibits reduced fatty acid oxidation, which may contribute to changes in total and regional body fat (*60*), whereas supplementation of E2 in OVX mice fed an HFD increases lipid oxidation and lipid utilization, thereby reducing obesity (*61*). Together, these results suggest that GPER activation by G-1 leads to reprogramming of WAT, enhancing fatty acid oxidation and alleviating hypoxia.

Estrogen deprivation results in mitochondrial dysfunction and altered lipid substrate use, with E2 supplementation reversing this effect (*62*). In the current study, G-1 treatment up-regulated the expression of mRNA for multiple mitochondrial and fatty acid oxidation proteins (*Ppargc1a*, *Acaca*, *Nrf1*, *Tfam*, and *Acox1*). In addition to WAT, other metabolically active tissues, such as BAT and skeletal muscle, also exhibited increased expression of these genes, which may further contribute to the increased energy expenditure and consumption of fuels. Furthermore, in vitro assays revealed that G-1 treatment enhanced both basal mitochondrial function and spare respiratory capacity, which reflects the vitality and survival capacity of cells (*63*). We did not observe an increase in proton leak in vitro as might be predicted from the increased expression of *Ucp1* in vivo, suggesting that the changes in *Ucp1* expression either require prolonged G-1 exposure or are not cell autonomous. Because G-1 also improves exercise capacity in OVX mice through the up-regulation of heat-shock proteins (*64*), G-1 preserves the function of metabolically critical tissues.

Rodents and primates, including humans, with increased body weight exhibit low-grade chronic inflammation in their WAT and other tissues due in part to ectopic fat deposition (*65*). Epidemiological data suggest that E2 has a protective role against chronic inflammatory diseases (*66*), because postmenopausal women exhibit increases in proinflammatory cytokines, an effect replicated in mice upon OVX (*67*). In the current study, G-1 treatment led to reduced plasma concentrations and expression of circulating and tissue inflammatory cytokines, consistent with previous studies in which loss of GPER results in increased systemic proinflammatory cytokines TNFα, MCP1, IL6, IL1β, and serum amyloid A3 (*25, 26*). A role for E2 and specifically GPER in the regulation of proinflammatory cytokines in adipocytes is suggested by studies using differentiated 3T3-L1 cells, where E2 treatment reduced proinflammatory gene expression, even after ERα knockdown, indicating an alternative pathway for E2 action, presumably via GPER (*68*). Direct evidence for the antiinflammatory actions of G-1 comes from studies of experimental autoimmune encephalomyelitis as a model of multiple sclerosis, in which G-1 reduced the severity of disease through reductions in proinflammatory activity (*69*). In other studies, G-1 promoted a regulatory T cell phenotype in proinflammatory T helper 17 cells through the induction of forkhead box P3 (Foxp3) and IL10 (*70, 71*). Thus, our results show that GPER activation by G-1 contributes to the maintenance of an antiinflammatory phenotype in vivo, which likely contributes to an improved metabolic phenotype.

Weight gain and obesity largely drive the increased prevalence of metabolic syndrome in postmenopausal women (and OVX mice) and in men. In mice and primates, including humans, the effects of hormone replacement therapy after menopause or E2 deficiency, leading to reduced visceral obesity and lower fasting serum glucose and insulin, indicate a protective role for E2 (*11*). Our results indicate that activation of GPER in OVX mice improves glucose tolerance with lower fasting glucose and insulin, and consequently a lower HOMA-IR, suggesting an improvement in peripheral insulin action to maintain glucose homeostasis. Furthermore, in our current study, male mice treated with G-1 also exhibited improved glucose tolerance with reduced insulin resistance in the absence of any weight loss. This result suggests a direct role for G-1 in modulating glucose homeostasis, consistent with previous reports, where both female and male mice fed an HFD displayed marked improvements in glucose homeostasis after E2 treatment (*48, 72*). GPER may improve glucose homeostasis in OVX mice through both direct effects on insulin producing pancreatic β cells or via actions on peripheral or central tissues (*73*). On the basis of our current results and published reports on the effects of GPER deficiency (*25, 26, 33*), we propose that the antiobesity and antidiabetic effects of G-1 in vivo involve both direct and indirect effects on multiple metabolic tissues such as the WAT, BAT, skeletal muscle, liver, and possibly pancreas to reduce obesity and improve glucose homeostasis.

Despite its extensive effects on metabolism, E2 is most widely appreciated as a potent regulator of reproductive tissues and bone health. E2 supplementation in OVX mice or after menopause in clinical studies restores bone health by maintaining, or reversing decreases in, bone mineral content and density (*74, 75*). However, unlike the established effects of E2 (*37*), in the current study, G-1 treatment did not yield any changes in bone mineral content or density. Furthermore, whereas E2 treatment of OVX mice leads to a rapid uterine imbibition response (the classic measure of "estrogenicity"), G-1 supplementation had no effect on uterine wet weight, as we have previously shown in both acute and chronic treatments (*28, 76*). Our results demonstrate that, although it restores normal body weight and metabolic function in E2-deficient mice, G-1 lacks the feminizing effects and bone mineral–preserving capacity of E2.

Limitations of this study include the use of mice to model human obesity and diabetes. In addition, given the complexity and interrelatedness of body weight regulation and glucose homeostasis involving multiple organ systems (including pancreas, liver, adipose, and muscle), ascertaining the primary direct versus secondary indirect effects of G-1, particularly in the OVX models where weight loss occurred in conjunction with improvements in glucose homeostasis, is challenging. Last, the efficacy and consequences (for example, potential toxicity) of long-term G-1 treatment, as would be required in humans to ameliorate obesity or diabetes, are currently unknown and require further preclinical and clinical studies.

In summary, this is the first study to demonstrate the beneficial metabolic effects of a GPER-selective agonist in vivo in both female and male mice. We show that G-1 exerts potent antiobesity and antidiabetic effects specifically through the stimulation of energy expenditure in the absence of effects on food intake or locomotor activity.

Our results could lead to therapeutic approaches against obesity and its associated metabolic consequences such as diabetes, not only in postmenopausal women but also in men. We conclude that G-1 is a bona fide first-in-class candidate prototype drug for potential translation into clinical applications. Future translational studies in men and women will ultimately establish the value of G-1 in obese and diabetic patients.

MATERIALS AND METHODS

Study design
The objective of this study was to determine the therapeutic potential of the GPER-selective agonist G-1 in preclinical mouse models of obesity and diabetes, including ovariectomy and high fat diet. Appropriate surgery, diet, and drug controls were included in the study. To reveal the mechanisms of G-1–mediated effects on metabolism, we performed studies on tissues or plasma obtained from various mouse cohorts. Power analyses were not used to calculate sample sizes; samples were not excluded, and investigators were not blinded during experiments. Before treatment, mice were weighed and assigned to treatment groups to ensure similar average initial body weights. About 12 to 14 mice were included in each treatment group, and body weights were monitored weekly throughout the treatment period. Mice were randomly selected for assessment of glucose homeostasis, body composition analysis, and metabolic parameters. At the end of the treatment period, in each treatment group, six of the mice were fasted before sacrifice with the remaining mice euthanized in a fed state. Plasma obtained from fasted mice was used for quantification of lipids, glucose, and insulin, whereas metabolic hormones and cytokines were assessed in plasma obtained from fed mice. Histology and gene expression studies were performed in tissues obtained from fed mice. Typically, four to eight mice (or derived samples such as plasma and tissue mRNA) were evaluated per condition. For in vitro metabolic studies, three independent experiments (with four replicates each) were performed, and representative results from one experiment are shown.

Animals, drug treatment, and tissue collection
C57BL/6 mice were obtained from Harlan Laboratories. Animals were housed at the Animal Resource Facility at the University of New Mexico Health Sciences Center. Animals were maintained under a controlled temperature of 22° to 23°C with 12-hour light and 12-hour dark cycle and fed a soy protein-free chow (defined as NC; 2920X, Envigo Corp.) ad libitum. All procedures were carried out in accordance with the National Institutes of Health (NIH) Guide for the Humane Care and Use of Laboratory Animals and approved by the University of New Mexico Institutional Animal Care and Use Committee as described (25). Female C57BL/6 mice were OVX at 10 weeks of age. Twelve weeks after OVX, animals were given subcutaneous injections of either vehicle (0.1% bovine serum albumin and 0.01% Tween 20 in 0.9% NaCl) or G-1 (200 μg) 3 days per week (Monday, Wednesday, and Friday) for 6 weeks. G-1, synthesized as described (77), was recrystallized from ethanol to obtain a diastereomerically pure, racemic mixture of syn-enantiomers. The identity of individual compound batches was verified by comparison of nuclear magnetic resonance (NMR) spectroscopy spectra to published values of ^{1}H NMR (400 MHz) δ and ^{13}C NMR (125 MHz) δ (77). Compound purity was demonstrated by high-field ^{1}H NMR and quantitative analytical high-performance liquid chromatography

to be >99%. For injections, a G-1 stock was prepared in ethanol and subsequently diluted into vehicle. For each treated animal, 200 μg of G-1 in 10 μl of ethanol (or ethanol alone as control) was diluted 10-fold in vehicle to a final volume of 100 μl. For the male DIO model, 6-week-old mice were switched to an HFD (TD.09766, Envigo Corp.) for 12 weeks before beginning treatment. Male mice received either vehicle or G-1 by subcutaneous injection as above, 5 days per week (Monday to Friday) for 8 weeks based on dose-finding experiments (figs. S5 and S6). A cohort of male mice fed NC served as an additional control. We further combined the effects of ovariectomy and an HFD in a female model of postmenopausal DIO, in which mice were OVX and switched to HFD at about 6 weeks of age, with ovary-intact mice as controls. After 12 weeks on the HFD, mice received either vehicle or G-1 by subcutaneous injection as above, 5 days per week (Monday to Friday) for 8 weeks. At the end of treatment period, animals were euthanized, blood and tissues were collected, and perigonadal and perirenal fat depots were carefully dissected and weighed. Perigonadal WAT, suprascapular BAT, skeletal muscle (gastrocnemius), and liver were collected and frozen for further analysis.

Body weight, food intake, locomotor activity, and energy expenditure
After the initiation of G-1 treatments, mice were weighed every week. For determination of food intake and energy expenditure, mice were placed in metabolic cages and acclimatized for 24 hours before obtaining data. All measurements were obtained using a computer-controlled indirect calorimetry system (Promethion, Sable Systems). Food consumption, oxygen consumption (VO_2), and carbon dioxide production (VCO_2) were measured. RER was derived as the ratio of VCO_2 to VO_2, indicating the primary fuel source used, whereas oxygen (O_2) consumption served as a measure of energy expenditure. Home cage locomotor activity was measured to assess activity in a nonaversive environment. Horizontal activity was automatically measured and recorded by photocell beam breaks using the PAS-Home Cage system (San Diego Instruments). Before data collection, mice were acclimatized in the chambers for 24 hours, after which data were collected for a subsequent 48 hours, including two complete light cycles (14 hours) and two complete dark cycles (10 hours). The animals had ad libitum access to the respective rodent chow and water during the study.

Body composition analysis
Changes in body composition were determined by performing DEXA and MRI scans on live animals from all mouse cohorts 2 to 4 days before euthanizing mice. DEXA scans were performed to determine bone mineral density, bone mineral content, body fat content, body fat percentage, and lean mass using a dedicated densitometer (Lunar Piximus II, Lunar Corporation, GE Medical Systems). This system uses a cone beam x-ray source generating energies of 35 and 80 keV and a flat 100 mm by 80 mm detector with individual pixel dimensions of 0.18 mm by 0.18 mm. A quality-control procedure was routinely performed with a calibration phantom before imaging. MRI images were obtained on a Biospec 4.7T (Bruker Corporation) with the following parameters: field of view, 4 cm by 4 cm; echo time, 13 ms; repetition time, 5000 ms; matrix, 256 by 256, as described (25). Images were analyzed for separation of fat/water content by the two-point Dixon method. Six coronal or axial sections per mouse from a similar body region were analyzed for total and subcutaneous fat content, respectively, using ImageJ software (https://imagej.nih.gov/nih-image).

Glucose and insulin tolerance tests

To assess the effect of GPER activation on metabolism, we performed GTTs and insulin tolerance tests (ITTs) as specified. Mice were fasted for 4 hours, and basal blood glucose (considered baseline) was measured. Subsequently, mice received glucose (2 g/kg body weight) or insulin (0.5 U/kg body weight) intraperitoneally. After injection, blood glucose was monitored at regular time intervals (15, 30, 60, and 120 min after administration) from tail nicks using the ReliOn Confirm glucose monitoring system (Relion Corp). Blood glucose was plotted as a function of time, and differences between treatment groups were assessed by the corresponding area under the curve (AUC).

Measurement of fasting plasma glucose, insulin, and lipids

Fasting glucose, insulin, cholesterol, and triglycerides were measured as described (25). Briefly, mice were fasted for 10 to 12 hours before euthanasia, and blood was collected by transthoracic cardiac puncture. Subsequently, glucose, insulin, triglycerides, and cholesterol (LDL and high-density lipoprotein) were measured in the plasma. Glucose was measured as above, and insulin was measured using a mouse insulin enzyme-linked immunosorbent assay kit (Mercodia AB). The extent of insulin resistance was quantified by the HOMA-IR using the matched fasting glucose and insulin concentrations. Total cholesterol and triglyceride concentrations were determined at IDEXX BioResearch.

Hematoxylin and eosin staining

After euthanasia, adipose tissue was rapidly fixed in phosphate-buffered saline (PBS) containing 4% paraformaldehyde (PFA) for 24 hours and subsequently washed with PBS and paraffin-embedded. Tissue sections (10 μm in thickness) were stained with hematoxylin and eosin (H&E). Images were quantified with ImageJ to derive relative adipocyte area in adipose sections.

RT-qPCR analysis

Total RNA was extracted from frozen perigonadal WAT, BAT, liver, and skeletal muscle (~30 to 50 mg) using the RNeasy Mini Kit (QIAGEN Co.). Isolated RNA (~100 ng) was used for complementary DNA (cDNA) synthesis using the ImProm-II Reverse Transcription System (Promega) in a final reaction volume of 20 μl. Subsequently, RT-qPCR was carried out in a 7500 Fast RT-PCR System (Applied Biosystems). Reactions for qPCR were set up in a total volume of 15 μl containing 7.5 μl Fast SYBR green Master Mix (Applied Sciences), 3.5 μl water, 1 μl forward and reverse primer (table S1) each (50 μM stock), and 2 μl cDNA for 40 cycles. Gene expression was normalized to *18S rRNA* as an internal reference, and fold change over the control was calculated using the $\Delta\Delta C_t$ method. qPCR reactions were performed in duplicate from a minimum of five individual mice.

Measurement of cellular respiration

Cellular respiration was measured as oxygen consumed in brown preadipocytes (78) using the XFe-24 analyzer (Agilent Technologies) according to the manufacturer's protocols. Cells were maintained in Dulbecco's modified Eagle's medium (DMEM) supplemented with 25 mM glucose, 2 mM glutamine, 10% fetal bovine serum, penicillin (100 U/ml), and streptomycin (100 μg/ml) in a humidified chamber at 37°C with 95% O_2 and 5% CO_2. Cells (50,000) were seeded in a 24-well plate, and after 24 hours, cells were starved in phenol-red free DMEM/F-12 medium supplemented with 5% charcoal-stripped serum.

The following day, cells were treated with either vehicle or 100 nM G-1 for 24 hours. On the day of analysis, the culture medium was removed, and cells were washed twice and switched to 500 μl of XF assay medium supplemented with 1 mM pyruvate, 2 mM glutamine, and 10 mM glucose (pH adjusted to 7.4) at 37°C in a CO_2-free incubator for 45 min before being transferred to the XFe analyzer for analysis of cellular respiration using the Mitochondrial Stress Test, in which cells are successively treated with the following modulators of mitochondrial function: oligomycin, FCCP, and rotenone/antimycin A. Cells were then fixed in PBS containing 2% PFA and quantified by crystal violet staining for normalization to cell numbers.

Measurement of mouse metabolic hormones and cytokines

Nonfasted mice were euthanized, and plasma samples collected. A mouse metabolic hormone magnetic bead panel (Millipore Corporation) was used to quantitate plasma amylin (active), C-peptide 2, ghrelin (active), GIP (total), GLP-1 (active), glucagon, IL6, insulin, leptin, MCP1, PP, PYY (total), resistin, and TNFα according to the manufacturer's instructions.

Statistical analysis

For each experiment, data were typically pooled from four to eight mice as indicated. Significance was determined by one-way analysis of variance (ANOVA) or two-way ANOVA with appropriate post hoc analyses using GraphPad Prism version 5.00 for Windows (GraphPad Software). For time-dependent body weight and cellular respiration studies, two-way ANOVA was used to compare between different mouse cohorts over time or treatment groups. For energy expenditure, locomotor activity, and GTT and ITT analyses, AUC was first calculated for each individual mouse, and different mouse cohorts were then compared by one-way ANOVA. Cellular respiration parameters were compared using the Mann-Whitney U test. $P < 0.05$ was considered statistically significant. Where P values are not provided in figures, statistically significant differences were not present.

SUPPLEMENTARY MATERIALS

View/request a protocol for this paper from *Bio-protocol*.

REFERENCES AND NOTES

1. E. Bojanowska, J. Ciosek, Can we selectively reduce appetite for energy-dense foods? An overview of pharmacological strategies for modification of food preference behavior. *Curr. Neuropharmacol.* **14**, 118–142 (2016).
2. N. Chevalier, P. Fenichel, Bisphenol A: Targeting metabolic tissues. *Rev. Endocr. Metab. Disord.* **16**, 299–309 (2015).
3. K. M. Flegal, D. Kruszon-Moran, M. D. Carroll, C. D. Fryar, C. L. Ogden, Trends in obesity among adults in the United States, 2005 to 2014. *JAMA* **315**, 2284–2291 (2016).
4. K. H. Saunders, D. Umashanker, L. I. Igel, R. B. Kumar, L. J. Aronne, Obesity pharmacotherapy. *Med. Clin. North Am.* **102**, 135–148 (2018).
5. M. G. Kolonin, P. K. Saha, L. Chan, R. Pasqualini, W. Arap, Reversal of obesity by targeted ablation of adipose tissue. *Nat. Med.* **10**, 625–632 (2004).
6. K. F. Barnhart, D. R. Christianson, P. W. Hanley, W. H. Driessen, B. J. Bernacky, W. B. Baze, S. Wen, M. Tian, J. Ma, M. G. Kolonin, P. K. Saha, K. A. Do, J. F. Hulvat, J. G. Gelovani, L. Chan,

Sharma *et al.*, *Sci. Transl. Med.* **12**, eaau5956 (2020)   29 January 2020

12 of 14

W. Arap, R. Pasqualini, A peptidomimetic targeting white fat causes weight loss and improved insulin resistance in obese monkeys. *Sci. Transl. Med.* **3**, 108ra112 (2011).

7. R. Pratley, A. Amod, S. T. Hoff, T. Kadowaki, I. Lingvay, M. Nauck, K. B. Pedersen, T. Saugstrup, J. J. Meier; PIONEER 4 investigators, Oral semaglutide versus subcutaneous liraglutide and placebo in type 2 diabetes (PIONEER 4): A randomised, double-blind, phase 3a trial. *Lancet* **394**, 39–50 (2019).

8. G. A. Christou, N. Katsiki, J. Blundell, G. Fruhbeck, D. N. Kiortsis, Semaglutide as a promising antiobesity drug. *Obes. Rev.* **20**, 805–815 (2019).

9. M. Rosenbaum, R. L. Leibel, Adaptive thermogenesis in humans. *Int. J. Obes. (Lond)* **34**(suppl. 1), S47–S55 (2010).

10. G. Srivastava, C. Apovian, Future pharmacotherapy for obesity: New anti-obesity drugs on the horizon. *Curr. Obes. Rep.* **7**, 147–161 (2018).

11. M. R. Meyer, D. J. Clegg, E. R. Prossnitz, M. Barton, Obesity, insulin resistance and diabetes: Sex differences and role of oestrogen receptors. *Acta Physiol (Oxf.)* **203**, 259–269 (2011).

12. B. J. Deroo, K. S. Korach, Estrogen receptors and human disease. *J. Clin. Invest.* **116**, 561–570 (2006).

13. E. R. Prossnitz, M. Barton, Estrogen biology: New insights into GPER function and clinical opportunities. *Mol. Cell. Endocrinol.* **389**, 71–83 (2014).

14. F. Mauvais-Jarvis, Sex differences in metabolic homeostasis, diabetes, and obesity. *Biol. Sex Differ.* **6**, 14 (2015).

15. R. P. Barros, J. Å. Gustafsson, Estrogen receptors and the metabolic network. *Cell Metab.* **14**, 289–299 (2011).

16. C. M. Revankar, D. F. Cimino, L. A. Sklar, J. B. Arterburn, E. R. Prossnitz, A transmembrane intracellular estrogen receptor mediates rapid cell signaling. *Science* **307**, 1625–1630 (2005).

17. E. Zekas, E. R. Prossnitz, Estrogen-mediated inactivation of FOXO3a by the G protein-coupled estrogen receptor GPER. *BMC Cancer* **15**, 702 (2015).

18. E. R. Prossnitz, J. B. Arterburn, H. O. Smith, T. I. Oprea, L. A. Sklar, H. J. Hathaway, Estrogen signaling through the transmembrane G protein–coupled receptor GPR30. *Annu. Rev. Physiol.* **70**, 165–190 (2008).

19. G. Sharma, E. R. Prossnitz, G-protein-coupled estrogen receptor (GPER) and sex-specific metabolic homeostasis. *Adv. Exp. Med. Biol.* **1043**, 427–453 (2017).

20. G. Sharma, F. Mauvais-Jarvis, E. R. Prossnitz, Roles of G protein-coupled estrogen receptor GPER in metabolic regulation. *J. Steroid Biochem. Mol. Biol.* **176**, 31–37 (2018).

21. G. Sharma, E. R. Prossnitz, GPER/GPR30 knockout mice: Effects of GPER on metabolism. *Methods Mol. Biol.* **1366**, 489–502 (2016).

22. M. Barton, E. R. Prossnitz, Emerging roles of GPER in diabetes and atherosclerosis. *Trends Endocrinol. Metab.* **26**, 185–192 (2015).

23. E. R. Prossnitz, L. A. Sklar, T. I. Oprea, J. B. Arterburn, GPR30: A novel therapeutic target in estrogen-related disease. *Trends Pharmacol. Sci.* **29**, 116–123 (2008).

24. M. R. Meyer, N. C. Fredette, T. Daniel, G. Sharma, K. Amann, J. B. Arterburn, M. Barton, E. R. Prossnitz, Obligatory role for GPER in cardiovascular aging and disease. *Sci. Signal.* **9**, ra105 (2016).

25. G. Sharma, C. Hu, J. L. Brigman, G. Zhu, H. J. Hathaway, E. R. Prossnitz, GPER deficiency in male mice results in insulin resistance, dyslipidemia, and a proinflammatory state. *Endocrinology* **154**, 4136–4145 (2013).

26. K. E. Davis, E. J. Carstens, B. G. Irani, L. M. Gent, L. M. Hahner, D. J. Clegg, Sexually dimorphic role of G protein-coupled estrogen receptor (GPER) in modulating energy homeostasis. *Horm. Behav.* **66**, 196–207 (2014).

27. C. G. Bologa, C. M. Revankar, S. M. Young, B. S. Edwards, J. B. Arterburn, A. S. Kiselyov, M. A. Parker, S. E. Tkachenko, N. P. Savchuck, L. A. Sklar, T. I. Oprea, E. R. Prossnitz, Virtual and biomolecular screening converge on a selective agonist for GPR30. *Nat. Chem. Biol.* **2**, 207–212 (2006).

28. M. K. Dennis, R. Burai, C. Ramesh, W. K. Petrie, S. N. Alcon, T. K. Nayak, C. G. Bologa, A. Leitao, E. Brailoiu, E. Deliu, N. J. Dun, L. A. Sklar, H. J. Hathaway, J. B. Arterburn, T. I. Oprea, E. R. Prossnitz, In vivo effects of a GPR30 antagonist. *Nat. Chem. Biol.* **5**, 421–427 (2009).

29. M. K. Dennis, A. S. Field, R. Burai, C. Ramesh, W. K. Petrie, C. G. Bologa, T. I. Oprea, Y. Yamaguchi, S. Hayashi, L. A. Sklar, H. J. Hathaway, J. B. Arterburn, E. R. Prossnitz, Identification of a GPER/GPR30 antagonist with improved estrogen receptor counterselectivity. *J. Steroid Biochem. Mol. Biol.* **127**, 358–366 (2011).

30. E. R. Prossnitz, J. B. Arterburn, International Union of Basic and Clinical Pharmacology. XCVII. G protein-coupled estrogen receptor and its pharmacologic modulators. *Pharmacol. Rev.* **67**, 505–540 (2015).

31. E. R. Prossnitz, GPER modulators: Opportunity Nox on the heels of a class Akt. *J. Steroid Biochem. Mol. Biol.* **176**, 73–81 (2018).

32. C. M. Revankar, C. G. Bologa, R. A. Pepermans, G. Sharma, W. K. Petrie, S. N. Alcon, A. S. Field, C. Ramesh, M. A. Parker, N. P. Savchuk, L. A. Sklar, H. J. Hathaway, J. B. Arterburn, T. I. Oprea, E. R. Prossnitz, A selective ligand for estrogen receptor proteins discriminates rapid and genomic signaling. *Cell Chem. Biol.* **26**, 1692–1702.e5 (2019).

33. E. Haas, I. Bhattacharya, E. Brailoiu, M. Damjanovic, G. C. Brailoiu, X. Gao, L. Mueller-Guerre, N. A. Marjon, A. Gut, R. Minotti, M. R. Meyer, K. Amann, E. Ammann, A. Perez-Dominguez,

M. Genoni, D. J. Clegg, N. J. Dun, T. C. Resta, E. R. Prossnitz, M. Barton, Regulatory role of G protein-coupled estrogen receptor for vascular function and obesity. *Circ. Res.* **104**, 288–291 (2009).

34. G. Sharma, E. R. Prossnitz, Mechanisms of estradiol-induced insulin secretion by the G protein-coupled estrogen receptor GPR30/GPER in pancreatic β-cells. *Endocrinology* **152**, 3030–3039 (2011).

35. U. E. Martensson, S. A. Salehi, S. Windahl, M. F. Gomez, K. Sward, J. Daszkiewicz-Nilsson, A. Wendt, N. Andersson, P. Hellstrand, P. O. Grande, C. Owman, C. J. Rosen, M. L. Adamo, I. Lundquist, P. Rorsman, B. O. Nilsson, C. Ohlsson, B. Olde, L. M. Leeb-Lundberg, Deletion of the G protein-coupled receptor 30 impairs glucose tolerance, reduces bone growth, increases blood pressure, and eliminates estradiol-stimulated insulin release in female mice. *Endocrinology* **150**, 687–698 (2009).

36. A. Wang, J. Luo, W. Moore, H. Alkhalidy, L. Wu, J. Zhang, W. Zhen, Y. Wang, D. J. Clegg, X. Bin, Z. Cheng, R. P. McMillan, M. W. Hulver, D. Liu, GPR30 regulates diet-induced adiposity in female mice and adipogenesis in vitro. *Sci. Rep.* **6**, 34302 (2016).

37. S. C. Garner, J. J. Anderson, M. H. Mar, I. Parikh, Estrogens reduce bone loss in the ovariectomized, lactating rat model. *Bone Miner.* **15**, 19–31 (1991).

38. J. C. Seidell, D. C. Muller, J. D. Sorkin, R. Andres, Fasting respiratory exchange ratio and resting metabolic rate as predictors of weight gain: The Baltimore Longitudinal Study on Aging. *Int. J. Obes. Relat. Metab. Disord.* **16**, 667–674 (1992).

39. J. Ye, Emerging role of adipose tissue hypoxia in obesity and insulin resistance. *Int. J. Obes. (Lond)* **33**, 54–66 (2009).

40. J. Yin, Z. Gao, Q. He, D. Zhou, Z. Guo, J. Ye, Role of hypoxia in obesity-induced disorders of glucose and lipid metabolism in adipose tissue. *Am. J. Physiol. Endocrinol. Metab.* **296**, E333–E342 (2009).

41. P. Trayhurn, Hypoxia and adipocyte physiology: Implications for adipose tissue dysfunction in obesity. *Annu. Rev. Nutr.* **34**, 207–236 (2014).

42. P. Seale, Transcriptional regulatory circuits controlling brown fat development and activation. *Diabetes* **64**, 2369–2375 (2015).

43. P. J. Havel, Update on adipocyte hormones: Regulation of energy balance and carbohydrate/lipid metabolism. *Diabetes* **53**(suppl 1), S143–S151 (2004).

44. M. E. Lean, D. Malkova, Altered gut and adipose tissue hormones in overweight and obese individuals: Cause or consequence? *Int. J. Obes. (Lond)* **40**, 622–632 (2016).

45. P. A. Heine, J. A. Taylor, G. A. Iwamoto, D. B. Lubahn, P. S. Cooke, Increased adipose tissue in male and female estrogen receptor-alpha knockout mice. *Proc. Natl. Acad. Sci. U.S.A.* **97**, 12729–12734 (2000).

46. V. Ribas, M. T. Nguyen, D. C. Henstridge, A. K. Nguyen, S. W. Beaven, M. J. Watt, A. L. Hevener, Impaired oxidative metabolism and inflammation are associated with insulin resistance in ERα-deficient mice. *Am. J. Physiol. Endocrinol. Metab.* **298**, E304–E319 (2010).

47. E. R. Prossnitz, H. J. Hathaway, What have we learned about GPER function in physiology and disease from knockout mice? *J. Steroid Biochem. Mol. Biol.* **153**, 114–126 (2015).

48. R. S. Dakin, B. R. Walker, J. R. Seckl, P. W. Hadoke, A. J. Drake, Estrogens protect male mice from obesity complications and influence glucocorticoid metabolism. *Int. J. Obes. (Lond)* **39**, 1539–1547 (2015).

49. R. D. Feldman, R. Gros, Q. Ding, Y. Hussain, M. R. Ban, A. D. McIntyre, R. A. Hegele, A common hypofunctional genetic variant of GPER is associated with increased blood pressure in women. *Br. J. Clin. Pharmacol.* **78**, 1441–1452 (2014).

50. D. Ricquier, Respiration uncoupling and metabolism in the control of energy expenditure. *Proc. Nutr. Soc.* **64**, 47–52 (2005).

51. W. Zhang, S. Bi, Hypothalamic regulation of brown adipose tissue thermogenesis and energy homeostasis. *Front. Endocrinol. (Lausanne)* **6**, 136 (2015).

52. A. Naaz, M. Zakroczymski, P. Heine, J. Taylor, P. Saunders, D. Lubahn, P. S. Cooke, Effect of ovariectomy on adipose tissue of mice in the absence of estrogen receptor alpha (ERα): A potential role for estrogen receptor beta (ERβ). *Horm. Metab. Res.* **34**, 758–763 (2002).

53. F. Lizcano, G. Guzmán, Estrogen deficiency and the origin of obesity during menopause. *Biomed. Res. Int.* **2014**, 757461 (2014).

54. R. Roberts, L. Hodson, A. L. Dennis, M. J. Neville, S. M. Humphreys, K. E. Harnden, K. J. Micklem, K. N. Frayn, Markers of de novo lipogenesis in adipose tissue: Associations with small adipocytes and insulin sensitivity in humans. *Diabetologia* **52**, 882–890 (2009).

55. J. H. Kim, M. S. Meyers, S. S. Khuder, S. L. Abdallah, H. T. Muturi, L. Russo, C. R. Tate, A. L. Hevener, S. M. Najjar, C. Leloup, F. Mauvais-Jarvis, Tissue-selective estrogen complexes with bazedoxifene prevent metabolic dysfunction in female mice. *Mol. Metab.* **3**, 177–190 (2014).

56. Q. Gao, T. L. Horvath, Cross-talk between estrogen and leptin signaling in the hypothalamus. *Am. J. Physiol. Endocrinol. Metab.* **294**, E817–E826 (2008).

57. D. J. Clegg, L. M. Brown, S. C. Woods, S. C. Benoit, Gonadal hormones determine sensitivity to central leptin and insulin. *Diabetes* **55**, 978–987 (2006).

58. K. M. Barnes, J. L. Miner, Role of resistin in insulin sensitivity in rodents and humans. *Curr. Protein Pept. Sci.* **10**, 96–107 (2009).

Sharma *et al.*, *Sci. Transl. Med.* **12**, eaau5956 (2020)   29 January 2020

13 of 14

59. B. A. Gower, T. R. Nagy, M. I. Goran, A. Smith, E. Kent, Leptin in postmenopausal women: Influence of hormone therapy, insulin, and fat distribution. *J. Clin. Endocrinol. Metab.* **85**, 1770–1775 (2000).

60. J. Abildgaard, A. T. Pedersen, C. J. Green, N. M. Harder-Lauridsen, T. P. Solomon, C. Thomsen, A. Juul, M. Pedersen, J. T. Pedersen, O. H. Mortensen, H. Pilegaard, B. K. Pedersen, B. Lindegaard, Menopause is associated with decreased whole body fat oxidation during exercise. *Am. J. Physiol. Endocrinol. Metab.* **304**, E1227–E1236 (2013).

61. J. Lee, J. M. Ellis, M. J. Wolfgang, Adipose fatty acid oxidation is required for thermogenesis and potentiates oxidative stress-induced inflammation. *Cell Rep.* **10**, 266–279 (2015).

62. J. P. Cavalcanti-de-Albuquerque, I. C. Salvador, E. L. Martins, D. Jardim-Messeder, J. P. Werneck-de-Castro, A. Galina, D. P. Carvalho, Role of estrogen on skeletal muscle mitochondrial function in ovariectomized rats: A time course study in different fiber types. *J. Appl. Physiol.* **116**, 779–789 (2014).

63. D. G. Nicholls, V. M. Darley-Usmar, M. Wu, P. B. Jensen, G. W. Rogers, D. A. Ferrick, Bioenergetic profile experiment using C2C12 myoblast cells. *J. Vis. Exp.* **2010**, 2511 (2010).

64. H. Wang, A. Alencar, M. Lin, X. Sun, R. T. Sudo, G. Zapata-Sudo, D. A. Lowe, L. Groban, Activation of GPR30 improves exercise capacity and skeletal muscle strength in senescent female Fischer344 × Brown Norway rats. *Biochem. Biophys. Res. Commun.* **475**, 81–86 (2016).

65. M. Longo, F. Zatterale, J. Naderi, L. Parrillo, P. Formisano, G. A. Raciti, F. Beguinot, C. Miele, Adipose tissue dysfunction as determinant of obesity-associated metabolic complications. *Int. J. Mol. Sci.* **20**, E2358 (2019).

66. R. H. Straub, The complex role of estrogens in inflammation. *Endocr. Rev.* **28**, 521–574 (2007).

67. A. Ludgero-Correia Jr., M. B. Aguila, C. A. Mandarim-de-Lacerda, T. S. Faria, Effects of high-fat diet on plasma lipids, adiposity, and inflammatory markers in ovariectomized C57BL/6 mice. *Nutrition* **28**, 316–323 (2012).

68. R. S. Santos, L. A. de Fatima, A. P. Frank, E. M. Carneiro, D. J. Clegg, The effects of 17 alpha-estradiol to inhibit inflammation in vitro. *Biol. Sex Differ.* **8**, 30 (2017).

69. E. Blasko, C. A. Haskell, S. Leung, G. Gualtieri, M. Halks-Miller, M. Mahmoudi, M. K. Dennis, E. R. Prossnitz, W. J. Karpus, R. Horuk, Beneficial role of the GPR30 agonist G-1 in an animal model of multiple sclerosis. *J. Neuroimmunol.* **214**, 67–77 (2009).

70. R. L. Brunsing, K. S. Owens, E. R. Prossnitz, The G protein-coupled estrogen receptor (GPER) agonist G-1 expands the regulatory T-cell population under TH17-polarizing conditions. *J. Immunother.* **36**, 190–196 (2013).

71. R. L. Brunsing, E. R. Prossnitz, Induction of interleukin-10 in the T helper type 17 effector population by the G protein coupled estrogen receptor (GPER) agonist G-1. *Immunology* **134**, 93–106 (2011).

72. J. P. Camporez, F. R. Jornayvaz, H. Y. Lee, S. Kanda, B. A. Guigni, M. Kahn, V. T. Samuel, C. R. Carvalho, K. F. Petersen, M. J. Jurczak, G. I. Shulman, Cellular mechanism by which estradiol protects female ovariectomized mice from high-fat diet-induced hepatic and muscle insulin resistance. *Endocrinology* **154**, 1021–1028 (2013).

73. R. Yonezawa, T. Wada, N. Matsumoto, M. Morita, K. Sawakawa, Y. Ishii, M. Sasahara, H. Tsuneki, S. Saito, T. Sasaoka, Central versus peripheral impact of estradiol on the impaired glucose metabolism in ovariectomized mice on a high-fat diet. *Am. J. Physiol. Endocrinol. Metab.* **303**, E445–E456 (2012).

74. U. I. Modder, B. L. Riggs, T. C. Spelsberg, D. G. Fraser, E. J. Atkinson, R. Arnold, S. Khosla, Dose-response of estrogen on bone versus the uterus in ovariectomized mice. *Eur. J. Endocrinol.* **151**, 503–510 (2004).

75. B. L. Riggs, The mechanisms of estrogen regulation of bone resorption. *J. Clin. Invest.* **106**, 1203–1204 (2000).

76. M. R. Meyer, N. C. Fredette, T. A. Howard, C. Hu, C. Ramesh, C. Daniel, K. Amann, J. B. Arterburn, M. Barton, E. R. Prossnitz, G protein-coupled estrogen receptor protects from atherosclerosis. *Sci. Rep.* **4**, 7564 (2014).

77. R. Burai, C. Ramesh, M. Shorty, R. Curpan, C. Bologa, L. A. Sklar, T. Oprea, E. R. Prossnitz, J. B. Arterburn, Highly efficient synthesis and characterization of the GPR30-selective agonist G-1 and related tetrahydroquinoline analogs. *Org. Biomol. Chem.* **8**, 2252–2259 (2010).

78. M. Liu, J. Bai, S. He, R. Villarreal, D. Hu, C. Zhang, X. Yang, H. Liang, T. J. Slaga, Y. Yu, Z. Zhou, J. Blenis, P. E. Scherer, L. Q. Dong, F. Liu, Grb10 promotes lipolysis and thermogenesis by phosphorylation-dependent feedback inhibition of mTORC1. *Cell Metab.* **19**, 967–980 (2014).

Citation: G. Sharma, C. Hu, D. I. Staquicini, J. L. Brigman, M. Liu, F. Mauvais-Jarvis, R. Pasqualini, W. Arap, J. B. Arterburn, H. J. Hathaway, E. R. Prossnitz, Preclinical efficacy of the GPER-selective agonist G-1 in mouse models of obesity and diabetes. *Sci. Transl. Med.* **12**, eaau5956 (2020).

Science Translational Medicine

Preclinical efficacy of the GPER-selective agonist G-1 in mouse models of obesity and diabetes

Geetanjali Sharma, Chelin Hu, Daniela I. Staquicini, Jonathan L. Brigman, Meilian Liu, Franck Mauvais-Jarvis, Renata Pasqualini, Wadih Arap, Jeffrey B. Arterburn, Helen J. Hathaway and Eric R. Prossnitz

Mimicking estrogen to target metabolism

Estrogen is known to have positive effects on obesity and metabolism. Here, Sharma *et al.* show that a small-molecule agonist of one of estrogen's receptors, the G protein–coupled estrogen receptor (GPER), may have a similar, but more targeted potential as a therapeutic in metabolic disease. In ovariectomized mice, a model of postmenopausal obesity, G-1 agonist treatment increased energy expenditure and had beneficial effects on weight, adiposity, metabolism, and inflammation. However, unlike traditional estrogen replacement therapy, GPER agonism did not affect bone density or result in uterine feminizing effects. G-1 also elicited weight loss in ovariectomized mice on a high-fat diet and prevented weight gain in obese male mice.

ARTICLE TOOLS	http://stm.sciencemag.org/content/12/528/eaau5956
SUPPLEMENTARY MATERIALS	http://stm.sciencemag.org/content/suppl/2020/01/27/12.528.eaau5956.DC1
RELATED CONTENT	http://stm.sciencemag.org/content/scitransmed/12/524/eaax6629.full http://stm.sciencemag.org/content/scitransmed/11/496/eaav1892.full http://stm.sciencemag.org/content/scitransmed/10/472/eaat3392.full http://stm.sciencemag.org/content/scitransmed/11/488/eaau7116.full http://stm.sciencemag.org/content/scitransmed/10/455/eaah6324.full http://stm.sciencemag.org/content/scitransmed/12/533/eaay8071.full http://stm.sciencemag.org/content/scitransmed/12/540/eaax9106.full http://stm.sciencemag.org/content/scitransmed/12/550/eaba6676.full http://stm.sciencemag.org/content/scitransmed/12/555/eaax8096.full http://stm.sciencemag.org/content/scitransmed/12/558/eaaz8664.full http://stm.sciencemag.org/content/scitransmed/12/571/eaay4145.full http://stm.sciencemag.org/content/scitransmed/13/584/eaaw9668.full http://stm.sciencemag.org/content/scitransmed/13/590/eabd6434.full
REFERENCES	This article cites 78 articles, 10 of which you can access for free http://stm.sciencemag.org/content/12/528/eaau5956#BIBL
PERMISSIONS	http://www.sciencemag.org/help/reprints-and-permissions

Use of this article is subject to the Terms of Service